Earth and Planetary Science Letters, 79 (1986) 120–132
Elsevier Science Publishers B.V., Amsterdam – Printed in The Netherlands

[5]

Lithospheric strength variations as a control on new plate boundaries: examples from the northern Red Sea region

Michael S. Steckler * and Uri S. ten Brink *,**

Lamont-Doherty Geological Observatory of Columbia University, Palisades, NY 10964 (U.S.A.)

Received October 31, 1985; revised version received May 5, 1986

The complex plate boundary between Arabia and Africa at the northern end of the Red Sea includes the Gulf of Suez rift and the Gulf of Aqaba–Dead Sea transform. Geologic evidence indicates that during the earliest phase of rifting the Red Sea propagated NNW towards the Mediterranean Sea creating the Gulf of Suez. Subsequently, the majority of the relative movement between the plates shifted eastward to the Dead Sea transform. We propose that an increase in the strength of the lithosphere across the Mediterranean continental margin acted as a barrier to the propagation of the rift. A new plate boundary, the Dead Sea transform formed along a zone of minimum strength. We present an analysis of lithospheric strength variations across the Mediterranean continental margin. The main factors controlling these variations are the geotherm, crustal thickness and composition, and sediment thickness. The analysis predicts a characteristic strength profile at continental margins which consists of a marked increase in strength seaward of the hinge zone and a strength minimum landward of the hinge zone. This strength profile also favors the creation of thin continental slivers such as the Levant west of the Dead Sea transform and the continental promontory containing Socotra Island at the mouth of the Gulf of Aden. Calculations of strength variations based on changes of crustal thickness, geotherm and sediment thickness can be extended to other geologic settings as well. They can explain the location of rerifting events at intracratonic basins, of backarc basins and of major continental strike-slip zones.

1. Introduction

The past two hundred million years of Earth history have been characterized by the breakup and dispersal of the Laurasia and Gondwana landmasses. Yet, little is known of the factors that determined the creation of new plate boundaries. It has been suggested that deep-seated or "active" asthenospheric processes control the position of new plate boundaries [1]. Alternatively, it has been proposed that large regional stresses arising from the motion of the lithospheric plates drive rifting [2]. In either case, the preferred location of the developing plate boundary deformation will follow zones of weakness [3]. Similarly, regions of high strength could act as barriers to the development of plate boundaries or as rigid blocks within a zone of deformation [4].

Vink et al. [5] considered strength differences between continents and oceans and concluded that continents are always weaker and will preferentially rift. However, a number of other factors such as geothermal gradients, radioactive heat generation, sediment thickness, and pre-existing bending moments need to be considered in analyzing strength variations in continents. We will demonstrate the importance of these factors by investigating the evolution of rifting at the northern end of the Red Sea.

2. Evolution of the northern Red Sea Rift

Rifting has been active in the Red Sea since the Oligocene and sea-floor spreading has been taking place in its southern part for the last 5 m.y. A well developed and generally fault bounded axial depression ~ 30 km wide is present in the northern Red Sea, but with only isolated intrusions and no evidence of sea-floor spreading [6]. Hence, the northern Red Sea is still in the late stages of continental rifting [7].

The Gulf of Suez is a northern arm of the Red Sea extending for over 300 km between Africa and the Sinai Peninsula. The width of the rift averages

* Order of authorship determined by coin toss.
** Also Department of Geological Sciences, Columbia University.

0012-821X/86/$03.50

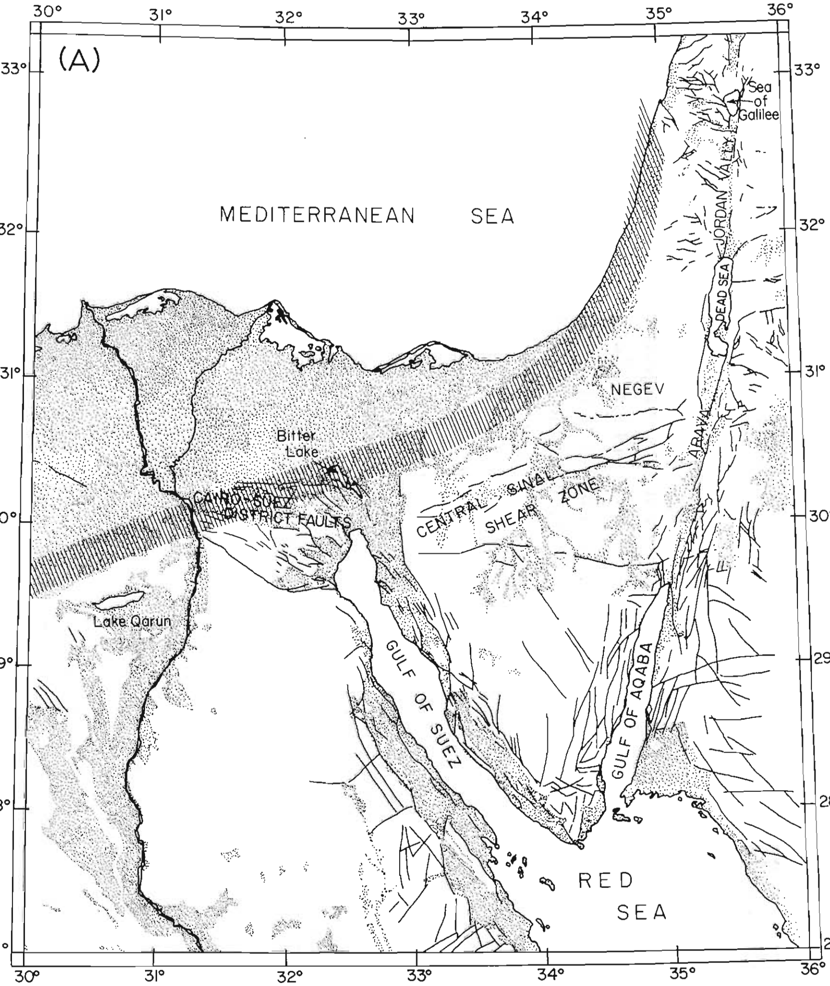

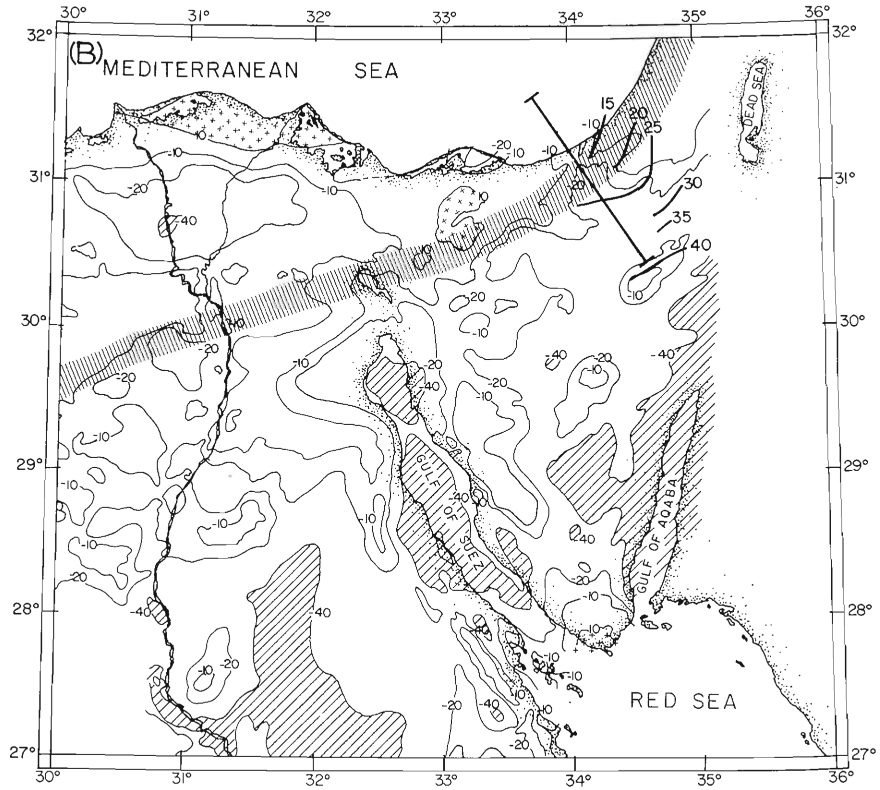

Fig. 1. A. Map of the Gulf of Suez region. Dotted pattern indicates location of Neogene and younger sediments, associated with the subsidence along the Gulf of Suez and Dead Sea Transform and the coastal plain cover along the Mediterranean continental margin. The hinge zone of the Mesozoic continental margin is shown by the hachures. Surface faults are indicated by the heavy lines. B. Bouguer gravity map of northeastern Egypt [37] and Sinai [38]. Merging of Egyptian and Sinai segments is approximate. The ENE trending anomalies are associated with the hinge zone. The large negative anomaly of the Gulf of Suez rift terminates south of the hinge zone. Heavy lines indicate location of profile given in Fig. 7 and contours of crustal thickness from seismic refraction [27].

~ 90 km. Except for an early phase of dike intrusion from 22 to 19 m.y. [8], there has been no igneous activity and extension has been accommodated by the rotation of tilted fault blocks. The main directions of faulting are N330° (the Clysmic trend parallel to the Gulf) and N10° (the Aqaba trend). Both of these trends may be related to pre-existing structures [9]. Steckler [10] estimated the total extension in the central Gulf of Suez as 25–27 km corresponding to an average extension factor (β) of 1.3. The amount of extension increases to the south. The high rift shoulders present in the south die out to the north and surface faulting cannot be traced north of the Bitter Lakes. At the termination of the rift, there is a splay of normal faults that extend westward towards Cairo and several long faults in central Sinai (Fig. 1).

Rifting in the Gulf of Suez began in the latest Oligocene/early Miocene (foram. zone N4-N5; [11]). The early phase of subsidence was characterized by open marine conditions with monotonous shale and mark deposition [12]. Backstripping of wells in the Gulf of Suez indicate 10–15 km of extension during this phase ([13]; Fig. 2).

A widespread unconformity, the Mid-Clysmic event at approximately 17 Ma [12,14] marks a dramatic change in tectonics in the Gulf of Suez. There is an angular discordance between the Upper and Lower Rudeis Formation, and a change from activity on many small faults to fewer larger ones [12]. The Upper Rudeis marks the beginning of major clastic input from the rift shoulders and shortly thereafter the continuing uplift of the rift shoulders isolated the Gulf of Suez and Red Sea from the Mediterranean Sea and evaporitic conditions developed (Fig. 2).

Normal marine conditions returned with the opening of an Indian Ocean portal through the southern Red Sea to the Gulf of Aden at the end of the Miocene. Backstripping reveals that during the post-Miocene, there is little net tectonic subsidence in the Gulf of Suez. However, because of the continued regional uplift [10,15] extension at this time cannot be ruled out by the lack of tectonic subsidence.

The Gulf of Aqaba–Dead Sea transform system branches off from the Red Sea–Gulf of Suez junction and has a total strike-slip offset of ~ 105 km [16]. Restoration of this motion aligns the eastern boundary faults of the Gulf of Suez and

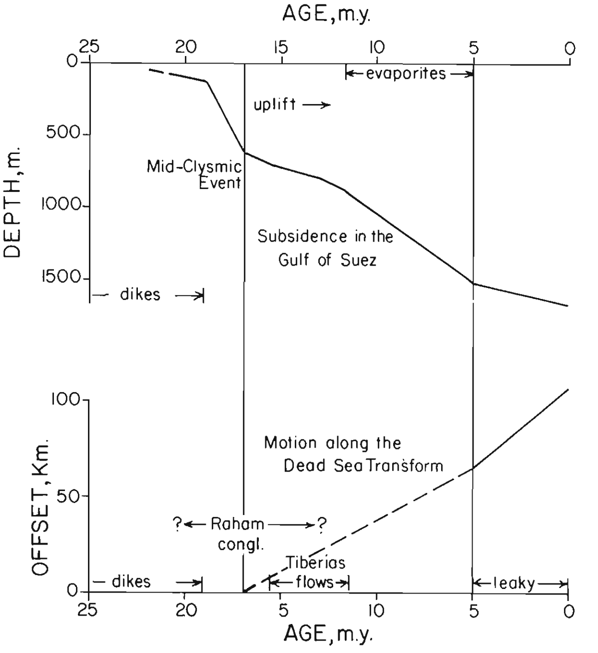

Fig. 2. Correlation of the tectonic development through time of the Gulf of Suez and Dead Sea Transform. Top shows tectonic subsidence in Gulf of Suez as deduced from backstripping of several wells in the central Gulf of Suez. Bottom indicates strike-slip motion along the Dead Sea Transform. Total offset is 105 km with 35–40 km of motion occurring in the last 5 m.y. Dashed line is extrapolation of strike-slip motion assuming its initiation correlates with mid-Clysmic event in Suez. See text for further explanation.

Red Sea. Projection of the Suez and Aqaba motions onto probable Red Sea opening directions indicate that 3/4 of the Africa-Arabian motion has been accommodated on the Gulf of Aqaba.

Movement in the Gulf of Aqaba post-dates the initial phases of motion in the Gulf of Suez–Red Sea as the faults in the Gulf of Aqaba offset Precambrian markers and the early Miocene dikes by the same amount [8,17]. Thus Gulf of Aqaba motion is younger than 19 Ma and post-dates the initial sediments in the Gulf of Suez. The Dead Sea Transform is also younger than the central Sinai shear zone which is offset by the 105 km of movement along the transform. The initiation of motion is probably no younger than the 15.5–11.5 m.y. old lower Tiberias basalt flows [8]. The Raham and Hazeva conglomerates represent the earliest exposed sediments related to motion on the Dead Sea transform. Exact ages cannot be established, but are presumed to be of Middle Miocene age

[18]. Although it cannot be directly correlated, it is possible that the initiation of the Dead Sea Transform corresponds in age to the Mid-Clysmic event. There is no evidence of activity along the Dead Sea transform prior to the Mid-Clysmic event. Furthermore, the reorganization of the fault blocks and the change in subsidence rates in the Gulf of Suez at this time is consistent with the changes expected from the development of a new plate boundary.

The initial movements along the Dead Sea Transform were nearly pure strike-slip [19]. In post-Miocene time, this motion changed to a leaky transform motion resulting in the opening of the grabens and half-grabens in the Dead Sea and Gulf of Aqaba [19,20]. Motion along the Dead Sea transform in this phase is estimated to be ~ 40 km [20]. This corresponds to ~ 35 km of extension in the direction perpendicular to the Gulf of Suez. As the total opening at the southern end of the Gulf of Suez is ~ 35 km, the Gulf of Aqaba–Dead Sea transform has been the primary plate boundary for the past 5 m.y.

To summarize, the existing geologic evidence on the timing of events in the Gulf of Suez and Aqaba, kinematic constraints and recent back-stripping results [13] indicate that the Gulf of Suez initiated prior to the Gulf of Aqaba as the northernmost part of the Red Sea. However, soon thereafter, the Gulf of Aqaba developed and supplanted the Gulf of Suez as the primary plate boundary between Arabia and Africa accommodating at least 75% of the plate motion north of the Red Sea.

3. Regional geologic setting

The basement of the Arabo-Nubian shield was assembled during the Pan-African orogenies (710–510 Ma) [21,22]. Minor igneous activity has continued sporadically throughout the Phanerozoic [23]. However, heat flow values in the interior of Egypt are low (42–47 mW/m^2; [24]) indicating a stable platform.

The other major structural province in this region is that of the Eastern Mediterranean. Interpretation of seismic refraction data from the Eastern Mediterranean [25] shows an unusually thick sedimentary section (10–14 km) overlying oceanic crust or thin stretched continental crust. The thinning of the continental crust underlying Egypt and the Levant northward and westward toward the Mediterranean along with thickening of the sedimentary cover are interpreted as a passive continental margin of the Arabo-Nubian platform [26,27]. Rifting in Israel and Sinai began during the Triassic with the deposition of clastic and evaporitic sediments in fault activated basins and erosion of local highs ([28]; ten Brink, unpublished manuscript, 1981). By the Pliensbachian (200–194 Ma), tectonic activity had stopped and widespread marine deposition was occurring. The wedge of late Liassic and younger sediments extend further landward than the Triassic, similar to the post-rift stratigraphic sequences at other continental margins [29]. A major basalt sequence in the subsurface of northern Israel is dated stratigraphically and radiometrically as Lower Jurassic [8,30]. Numerous intrusions and extrusions continued during the Jurassic and into the Cretaceous [31] throughout the region.

A major feature of continental margins is the hinge zone [32] marking the beginning of the region which underwent substantial extension during rifting. The Mesozoic hinge zone in Egypt and Israel is shown in Fig. 1. The position of the hinge zone was located using surface and subsurface geology, seismic refraction data, and the magnetic and gravity fields [25,27,28,33–38]. At the hinge zone, there is a rapid increase in sediment thickness especially of Jurassic age, and decrease of crustal thickness.

The northernmost surface expression of Gulf of Suez rift dies out to the north and does not cross the Mesozoic hinge zone (Fig. 1). The Dead Sea transform is always landward of the hinge zone where it can be mapped. In the segment between the Dead Sea and the Sea of Galilee, it maintains a fairly constant distance east of the hinge zone. Thus, it appears that the Neogene rift does not propagate seaward through the hinge zone. The plate boundary preferentially follows a continental path by continuing further east.

4. Strength of the lithosphere

The development of a plate boundary requires the lithosphere to fail mechanically throughout its thickness. The yield stress envelope describes the stresses at which mechanical failure occurs [39].

Therefore, the integrated area of the yield stress envelope is taken as a representative measure of the force needed to induce rifting.

A yield stress envelope in tension for oceanic and continental lithosphere is shown in Fig. 3B. A linear frictional law known as Byerlee's law determines the failure stress in the brittle portions of the curves where strength increases with depth [40]. This law is independent of rock type. The differences between the oceanic and continental curves is due to the variation in overburden of the respective crusts.

The portions of the curves where the strength decreases with depth is controlled by ductile flow laws which are strain rate, stress and highly temperature dependent. The geotherms used to calculate the ductile flow are shown in Fig. 3A. They correspond to 200 m.y. old lithosphere with an equilibrium thermal thickness of 125 km. We choose 200 m.y. as an approximate age for the formation of the hinge zone in the Eastern Mediterranean. The difference in geotherms is due to radiogenic heat production in the continental crust. We use the flow laws for olivine given by Goetze [41] for the lowermost part of the yield envelopes

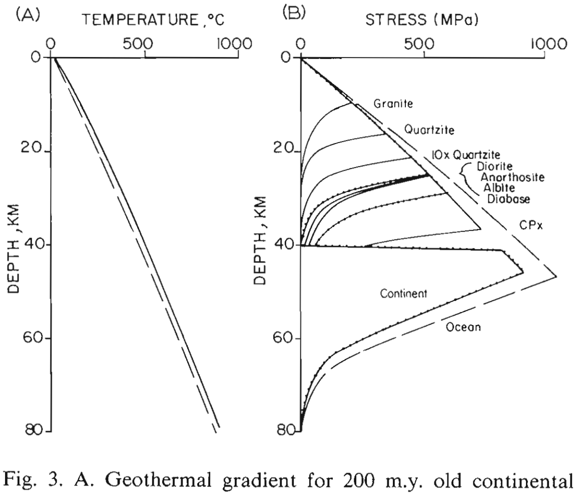

Fig. 3. A. Geothermal gradient for 200 m.y. old continental (solid) and oceanic (dashed) lithosphere with an equilibrium thermal thickness of 125 km. Radiogenic heat production in the continental crust is 1.7 exp($-z/10$ km) $\mu W/m^2$ where z is depth. B. Yield stress envelopes in tension for continental (solid) and oceanic (dashed) lithospheres with geotherms given in (a) for a strain rate of 10^{-15} s^{-1}. Different continental envelopes in the crust correspond to rheologies for different crustal compositions as labeled. The dotted lines correspond to the range of rheologies used for model calculations.

which is entirely within the mantle. The yield stress envelope in the oceans is entirely determined by Byerlee's law and the olivine flow law [39,42].

Ductile flow in the more siliceous rocks occurs at a lower-temperature range than olivine and is, therefore, expected to take place within the thick continental crust. Under geologic conditions, clinopyroxene will flow at 400–500°C and granite at 250–300°C compared to olivine which flows at 700–800°C. Ductile flow laws given by Kirby [40] for a variety of crustal materials are plotted in Fig. 3B. In this paper, we use the range of mafic rheologies from diorite to diabase, marked by the dotted lines, representative for the whole crust.

As can be seen, continental lithosphere is weaker than oceanic lithosphere of the same age. This is mainly due to the low strength in the lower crust. We use a 40 km thick continental crust following the refraction results on the Arabo-Nubian shield [34,43]. It is evident from the figure that the thickness of the crust is a major control on the strength of the lithosphere. This has led Vink et al. [5] to conclude that continents will always be weaker than the oceans. However, this conclusion depends on the geotherms in the ocean and continent being the same.

Fig. 4 plots the total integrated strength of the yield envelope versus age of the lithosphere. The

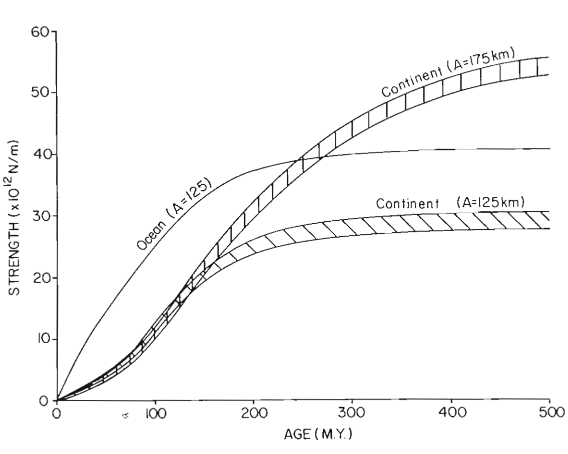

Fig. 4. Total integrated strength of the yield stress envelope in tension versus age of the lithosphere. Hachured area spans the range in strength calculated for the rheologies dotted in Fig. 3B. Geotherms were calculated using the plate model for lithospheric thicknesses ($A = 125$ or 175) as given.

oceanic curve shows the increasing strength of the yield envelope as the oceanic lithosphere cools and ages. The strength reaches a constant value as the lithosphere asymptotically approaches its equilibrium thermal thickness of 125 km. If the same lithospheric thermal thickness is assumed for the continent, then at the same age or geotherm the continent will always be weaker. However, an old continent can be stronger than a young ocean. Also, if some parts of the continents have a larger equilibrium thermal thickness [44], then their strength could be larger than old oceans. Illustrated in Fig. 4 is the case of a 175 km thick continental lithosphere. Its larger strength at old ages is due to lower geothermal gradient. The slight differences in the two continental curves at young ages (< 100 m.y.) is due to variations in the assumed radiogenic heat production. Since the partition of heat flux between radiogenic and mantle components is not known for the Nubian shield, the radiogenic flux was varied to insure consistency with the measured surface heat flux in Egypt [24].

An additional major factor that can modify the strength of the lithosphere is the sediment thickness. At continental margins, sediment thicknesses can reach 10 km or more. Fig. 5 illustrates the weakening of oceanic lithosphere due to 10 km of sediment cover. We assume that the porosity decreases exponentially with depth and that the pore pressure is hydrostatic in the sediment. The strength of the brittle part of the yield stress envelope is decreased due to the lower overburden of the low-density sediments. The strength of the ductile part is also decreased due to the high temperatures in the crystalline basement caused by the lower conductivity of the sediments. The net result is a 13% decrease in the total area of the yield envelope which, as will be shown, is a significant variation in terms of strain rate. Large sediment loads will have a larger effect on the strength of continental lithosphere since the increased temperatures with the downward displacement of the lithosphere will cause additional yielding in the crust. The contribution of the sedimentary cover to the weakening of the lithosphere is an important feature which has not been considered by previous studies.

The age of Eastern Mediterranean continental margin is about 200 m.y. At this age as shown by

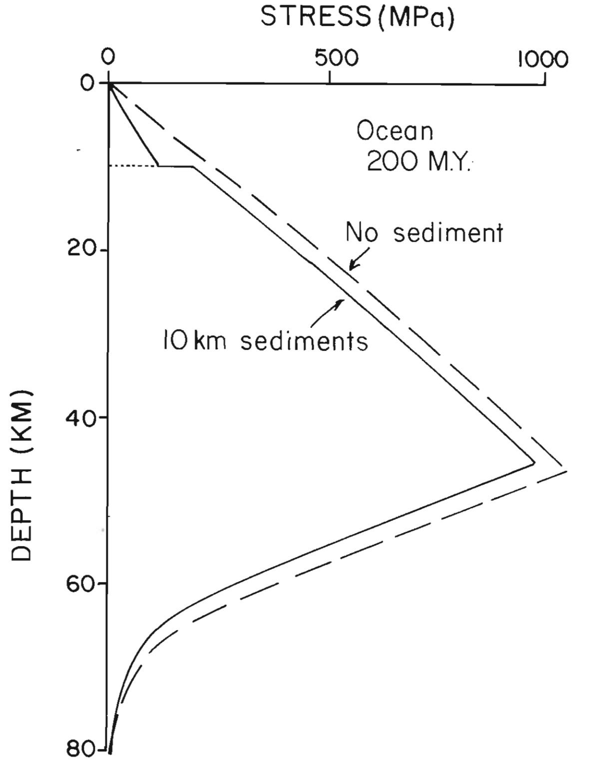

Fig. 5. Comparison of yield stress envelopes for oceanic lithosphere without sediments and loaded with 10 km of sediments. Porosity (ϕ) of the sediments decreases exponentially with depth according to the relation $\phi = 0.6 \exp(-z/2 \text{ km})$. Conductivity varies linearly with porosity with conductivities of 1.5 and 2.7 mW/°C-M for water and the average sediment composition. Sediment grain density of 2.68 g/cm^3. Yield envelopes were calculated with a strain rate of 10^{-15} s^{-1}.

Fig. 4, the oceanic lithosphere is stronger than the continental by 14–21% (175 km lithosphere) to 30–37% (125 km lithosphere). Are these strength differences large enough to control the location of rifts?

The strength of the lithosphere represents the force needed to induce rifting. Because of the power law form of the ductile flow laws, the strength of the lithosphere is strain rate dependent. Fig. 6 shows the strength of lithosphere as a function of strain rate. The curves indicate that the force needed to rift the lithosphere is only slightly smaller for deformation proceeding at a much slower rate. Although the strength of the oceans is not much larger than that of continents, an applied force which is capable of rifting con-

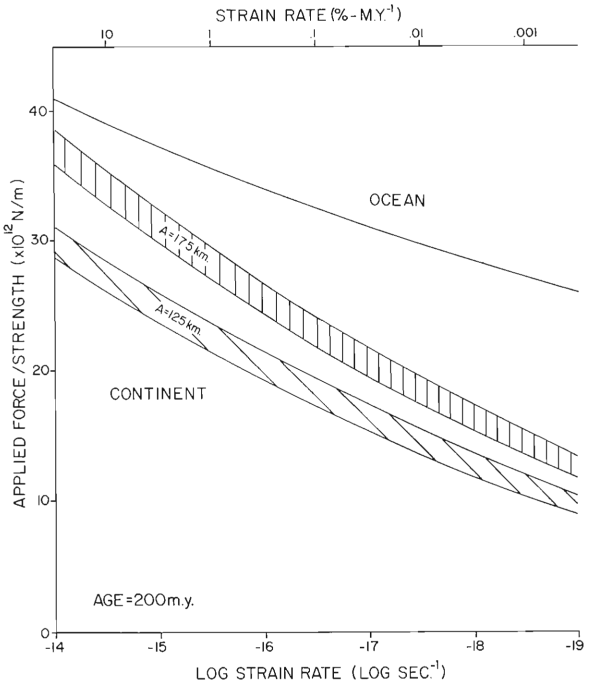

Fig. 6. Variation in strength of the oceanic and continental lithosphere versus log strain rate. Note that for a given applied force, the strain rate in oceanic lithosphere is several orders of magnitude lower.

tinental lithosphere at geological rates will rift oceans at a rate of 2–3.5 orders of magnitudes slower. This implies that propagation of a rift from continent to ocean causes deformation rate to drop from geologically reasonable levels (30–0.3% m.y.$^{-1}$ or 10^{-14}–10^{-16} s^{-1}), to negligible levels. This will be true not only when the two regions are continent and ocean, but also for two adjacent continental regions of different strengths.

5. Implications for the northern Red Sea

A profile based on seismic refraction and surface and subsurface data [27] across the margin at the southeastern corner of the Mediterranean is shown in Fig. 7A (see Fig. 1B for location). The profile has been extended landward as it would have been prior to initiation of the Neogene rifts. The corresponding strength profile is shown in Fig. 7B and yield stress envelopes for several positions along the profile are given in Fig. 7C. The hachured area in the strength profile corresponds to the range of crustal rheology from diorite to diabase. The strength profile was calculated using a geotherm for lithosphere 200 m.y. after rifting including extensive heating well landward of the hinge zone (> 100 km) in accord with recent results [10,45]. Radiogenic heat sources were thinned with the crust. The lithospheric thickening towards the center of the Arabo-Nubian shield is unknown and we have, therefore, indicated a possible increase in the upper bound of the strength profile towards a lithosphere of 175 km thickness and an age of 500 m.y. Sediment compaction parameters increase linearly seaward across the margin with surface porosity and characteristic compaction depth varying from 0.5 to 0.7 and 1 km to 2.5 km, respectively [45]. A surface temperature of 20°C was used on land and 13°C (Mediterranean bottom water temperature) offshore.

The calculated strength profile shows large variations in strength in the region. In particular, a sharp increase in strength occurs in a zone 60 km wide where the crust thins by 25%. In the absence of sediments, the strength increase would be even larger. A minimum in strength occurs at $x = 160$ km where the crust attains its full thickness.

The changes in strength can be explained by examining the yield stress envelopes in Fig. 7C. The rapid increase in strength from $x = 160$ km to $x = 120$ km is due to the decreasing crustal thickness in accord with observation that Triassic rifting extends as far landward as Har Loz ($x = 150$). The crustal thinning has the effect of replacing low strength crustal rocks with higher strength mantle rocks. This first 25% of the crustal thinning removes the bulk of the "bite" introduced into the yield envelope by the crustal rheology. By $x = 60$ km, the weak zone in the crust is entirely gone. The increasing strength with crustal thinning is partially offset by the weakening due to the increasing sediment thickness. Seaward of $x = 30$ km, this actually causes a slight decrease in total strength.

The strength increase landward of $x = 160$ km is caused by two factors, the pinchout of the flexural sediment wedge and the decrease in geotherm away from the continental margin. The strength minimum would be more pronounced in a younger continental margin where the heat flux would be greater.

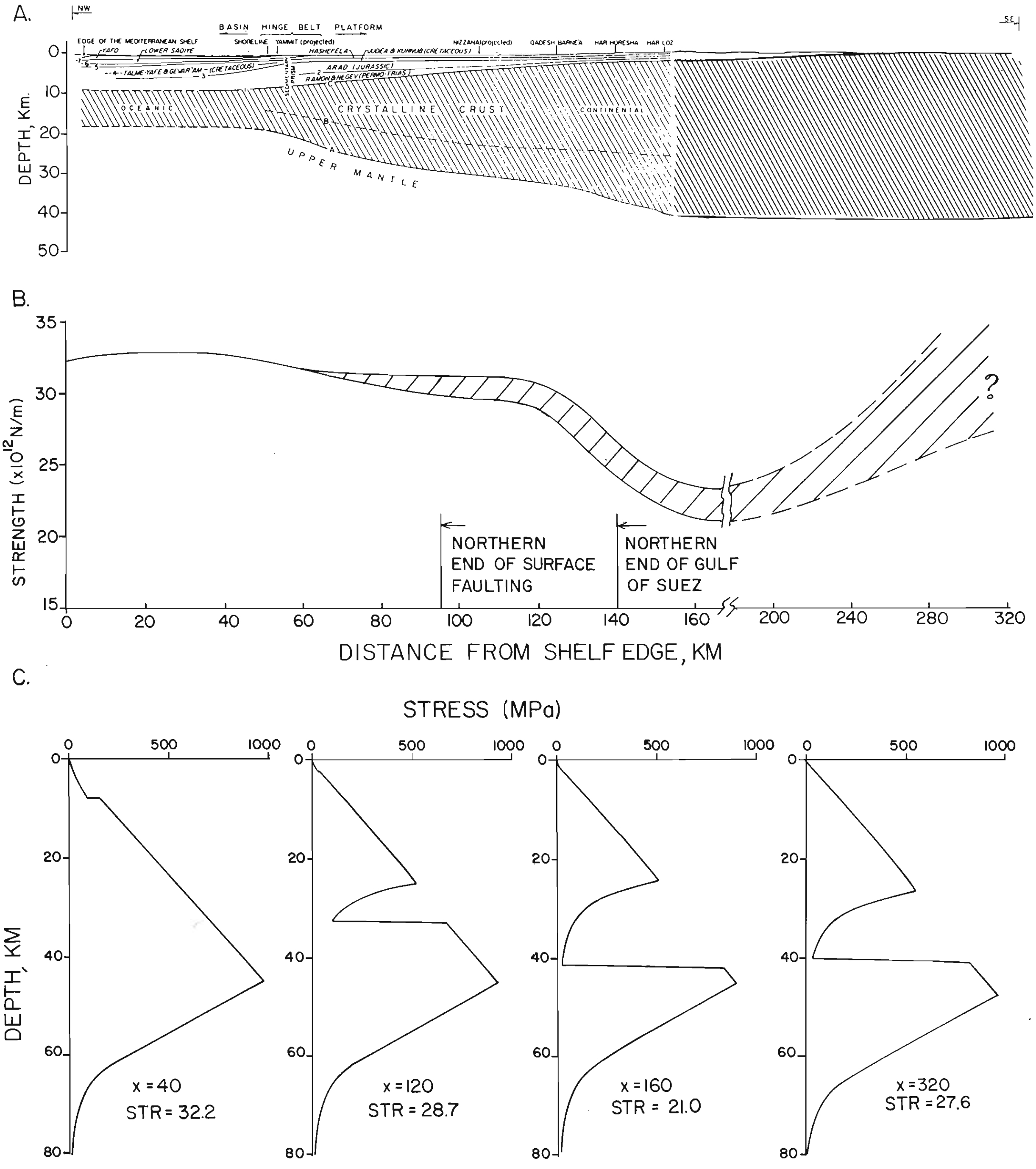

Fig. 7. A. Profile across Mediterranean continental margin given by Ginzburg and Gvirtzman [27]. Location is shown in Fig. 1B. Profile has been extrapolated southwards 160 km using pre-Gulf of Aqaba sediment and crustal thicknesses. B. Variation of total lithospheric strength along profile. The effects of changing crustal thickness, sediment thickness and geotherm have been included. Hachured region between solid lines bounds the strengths calculated for the two dotted crustal compositions in Fig. 3B. Dashed lines reflect the uncertainty in lithospheric thickness (125–175 km thick) of Arabo-Nubian shield. Relative position of the northern terminus of Gulf of Suez is indicated. Note change in scale at $X = 160$ km. C. Yield stress envelopes for several positions along profile. Position (km) and strength ($\times 10^{12}$ N m^{-1}) are indicated for each yield envelope. Note the removal of the low strength zone in the lower crust and the effects of the geotherm and sediments.

The sharp increase in the strength of the lithosphere across the continental margin may have acted as a barrier to the propagation of the Gulf of Suez into the Mediterranean. Indeed, as shown in the gravity map of Fig. 1B, rifting in the Gulf of Suez does not penetrate the hinge zone. Fig. 7B indicates the location of the termination of the Gulf of Suez with respect to the strength profile. The major expression of the rift dies out as the strength begins to increase. All surface faulting disappears at the hinge zone. Furthermore, the faulting in the Cairo–Suez district and central Sinai are also confined landward of the hinge zone (Fig. 1A).

The segment of the Dead Sea transform from the Dead Sea to the sea of Galilee is located at the minimum of the strength profile. This explains why the trend of the rift valley formed subparallel to the older structures and isopachs of the continental margin. The crust in Jordan immediately east of the rift valley is unthinned (40 km thick; K. Fuchs, personal communication, 1985) while west of the rift valley, it shows the Mesozoic thinning [46].

We, therefore, envision the following scenario for the evolution of the plate boundary in the northern Red Sea region. Red Sea rifting initially propagated up the Gulf of Suez until it reached the hinge zone of the Mesozoic continental margin. The development of the Cairo–Suez district faulting and central Sinai shear zone followed a region of minimum strength lying landward of the hinge zone. The new plate boundary eventually continued northwards along the Dead Sea transform. This model predicts that the transform initiated in the Dead Sea–Hula Valley segment where the transform parallels the earlier margin. It then connected to the Red Sea along the Gulf of Aqaba and the Arava Valley. This connection is preferred over the central Sinai shear zone because motion in the central Sinai would have been transpressional while the Gulf of Aqaba motion was pure strike-slip. The strength of rocks under compression is much greater than for strike-slip or extension. Also field evidence in the Eastern Desert of Egypt shows that the Gulf of Aqaba trend was a preexisting structural trend (K. Gerdes, personal communication, 1986). Furthermore, the Gulf of Aqaba was already thermally perturbed by a zone of dikes related to the development of the Red Sea. Once the Gulf of Aqaba developed, the majority of motion took place along the Dead Sea transform.

6. Application to the Gulf of Aden

The Eastern Mediterranean plate boundary is but one example of the tectonic control of the hinge zone. At the other end of the Red Sea, opening of the Gulf of Aden seems to be influenced by the earlier continental margin. Fig. 8 shows that the propagation of rifting from the Carlsberg Ridge towards the Afar did not follow the shortest path. Rather, it deviated to the north along the Owen Fracture Zone taking a longer path and creating the continental promontory of

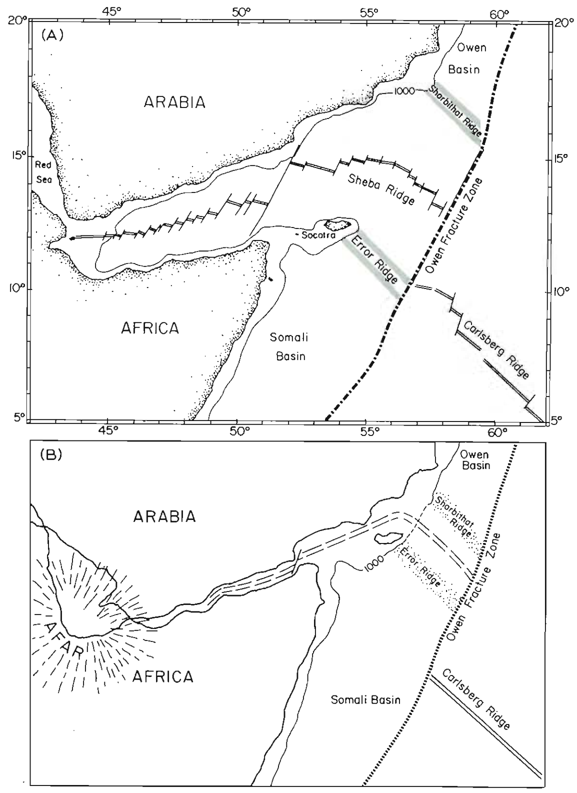

Fig. 8. A. Map of the plate boundaries and tectonic features of Gulf of Aden. Separation of Arabia and Africa created continental promontory around the island of Socotra. Error and Sharbithat ridges are of uncertain origin. B. Reconstruction of Gulf of Aden [65] shows circuitous path of the rift propagating from Carlsberg ridge to the Afar. The rift avoids the Somali Basin and then continues parallel to continental margin creating the continental promontory.

Socotra Island. The reconstruction of the region prior to opening the Gulf of Aden (Fig. 8B) shows the relationship of the rifting to the continental margin. The rifting avoids going through the Somali Basin which is thought to be at least mid-Jurassic in age (J.R. Cochran, personal communication, 1985). Instead it develops 300 km to the north where the Owen Fracture Zone is closer to the Arabian continental margin. The rift divides the Sharbithat and Error Ridges which may be either constructural features created during rifting or pre-existing structures [47], possibly of continental origin (D. McKenzie, personal communication, 1985). It continues parallel and landward of the continental margin for over 450 km to the Alula-Fartak Fracture Zone. The rift then propagates inland to the pre-existing thermal anomaly of Afar.

The longer, more circuitous route is a result of the variations in strength in the region. The lithosphere of the Somali and Owen Basins is expected to be stronger than the Arabian continental margin. The longer route is the easiest to break. The northern detour of rifting would be even more favored if the Sharbithat and Error Ridges were an already existing structure.

7. Discussion

The variation in strength of the lithosphere appears to be a major control in the development of plate boundaries. Our analysis used conservative estimates of the variation in strength of the lithosphere. We used a uniform mafic composition for the continental crust although granites are widely exposed in the Nubian shield. Yield stress envelopes constructed for continental lithosphere have usually used a quartz rheology for the entire crust [5,48]. Other authors have used a multiple layered crust with the upper crust composed of quartz [49,51]. Yet others have totally ignored the strength of the crust altogether [52,53]. Using these rheologies this would greatly increase the strength variation due to changing crustal thickness.

The flexural bending which occurs at continental margins contributes to weakening of parts of the margin. The bending moment due to the sediment loading decreases the strength of the yield envelope and, therefore, lower axial forces are needed to break the lithosphere. This flexural effect will be maximal beneath (1) the sediment load and (2) halfway to the axis of the outer high with a minimum in between. The location of the second maximum in the Levant margin may lie close to the zone of minimum strength in Fig. 7. Flexural bending will have little effect when rifting is perpendicular to the margin as in the Gulf of Suez, but may be a factor in determining the location of rifting parallel to a margin as in the Dead Sea transform and the Gulf of Aden. When the factors considered above are taken into account, the variation in strength across a margin are likely to be larger than we have estimated.

At a continental margin the weakest site will generally be landward of the hinge zone, as in the cases of the Levant and Gulf of Aden. This provides a mechanism for creating thin slivers of continental crust as in the Seychelles, Rockall Plateau, Lomonosov Ridge [5], Norfolk Ridge, Dampier Ridge, and Lord Howe Rise [54] which may ultimately end up as exotic terranes.

Crustal thinning, sediment accumulation and heating is not confined to continental margins, but also occurs at intracratonic rift basins. Reactivation of these rift basins may take place to the side of the old rifts where crustal thickness is larger. Rerifting to the side of the Mesozoic intracratonic basin off Norway created the North Atlantic Ocean and left the Vöring Plateau behind [55]. Reactivation will take place within the rifted basin if the sediment thickness and/or geotherm are higher. Jurassic rifting in the Central Graben of the North Sea occurs asymmetrically within the Permo-Triassic basin [56].

Calculations of strength variations based on changes in crustal thickness, geotherm and sediment thickness can be extended to other tectonic settings. When the sense of motion at a plate boundary changes from subduction to strike-slip, the plate boundary moves inland. Examples of this include the Fairweather and Queen Charlotte Faults in Canada and Alaska [57] and the San Andreas Fault system in California [58]. Further south, the oblique opening of the Gulf of California took place inland from the subduction zone at the volcanic arc. The thicker crust and elevated geotherm at this site indicate that it would have been the weakest lithosphere.

Fitch [59] has shown that oblique subduction will decouple into normal subduction and strike-slip. Our model predicts that the preferred location of the strike-slip motion will be at the weakest lithosphere, generally near the volcanic arc (e.g. Sumatra [60]; Western Aleutians [61]). Backarc spreading, as in the Andaman Sea [62] Lau-Havre Trough and Philippine Sea [63] initiates in this location.

In more complex cases of convergence, transforms will develop at the site of the weakest lithosphere. The collision between Arabia and Anatolia is accommodated by the westward expulsion of Turkey. The North Anatolian Fault, which parallels the southern coast of the Black Sea, forms the northern boundary of the deforming region. The thicker continental crust of the Anatolian block is weaker than the Black Sea which is thought to be a remnant of old oceanic or thin stretched continental lithosphere [64].

In summary, variations in the strength of the lithosphere can be a major control on the development of new plate boundaries. The main factors contributing to changes in strength of different provinces are the crustal thickness and composition, the geotherm, and thickness of the overlying sediments. Together they produce a characteristic strength profile across continental margins. This strength profile shows a marked increase in strength across the hinge zone and a zone of minimum strength immediately landward. The location and magnitude of these features will strongly depend upon age and geometry of the margin. In the Gulf of Suez, the change in strength hindered the northward propagation of the rift. The Dead Sea transform accommodated the relative motion of Africa and Arabia further north by utilizing the weak zone parallel to the Mediterranean margin. This variation in strength across a continental margin provides a mechanism for creating thin continental slivers. Application of yield strength analysis to other tectonic settings can explain the locations of many extensional and transform features.

Acknowledgements

J. Weissel, P. Morgan, Z. Garfunkel, A.B. Watts, M. McNutt and C.G.A. Harrison reviewed the manuscript and provided helpful comments. We wish to thank GUPCO and AMOCO for the release of data used in this paper. This work was supported by NSF grants OCE 83-09983 and OCE 85-14073 and a grant from Texaco. Lamont-Doherty Geological Observatory contribution number 3958.

References

1 J.F. Dewey, and K. Burke, Hot spots and continental breakup, Geology, pp. 57–60, 1974.
2 A.M.C. Sengör and K. Burke, Relative timing of rifting and volcanism on Earth and its tectonic implications, Geophys. Res. Lett. 5, 419–421, 1978.
3 L.R. Sykes, Intraplate seismicity, reactivation of preexisting zones of weakness, alkaline magmatism and other tectonism postdating continental fragmentation, Rev. Geophys. Space Phys. 16, 621–688, 1978.
4 J. Jackson and D.P. McKenzie, Active tectonics of the Alpine-Himalayan belt between western Turkey and Pakistan, Geophys. J. R. Astron. Soc. 77, 185–264, 1984.
5 G.E. Vink, W.J. Morgan and W.-L. Zhao, Preferential rifting of continents: a source of displaced terranes, J. Geophys. Res. 89, 10072–10076, 1984.
6 J.R. Cochran, F. Martinez, M.S. Steckler and M. Hobart, Conrad Deep: a new northern Red Sea Deep, origin and implications for continental rifting, Earth Planet. Sci. Lett., 78, 18–32, 1986.
7 J.R. Cochran, A model for the development of the Red Sea, Am. Assoc. Pet. Geol. Bull. 67, 41–69, 1983.
8 G. Steinitz, Y. Bartov and J.C. Hunziker, K-Ar age determinations of some Miocene-Pliocene basalts in Israel: their significance to the tectonics of the Rift Valley, Geol. Mag. 115, 329–340, 1978.
9 D.A. Robson, The structure of the Gulf of Suez (Clysmic) rift, with special reference to the eastern side, London Q. J. Geol. Soc. 115, 247–276, 1971.
10 M.S. Steckler, Uplift and extension at the Gulf of Suez—indications of induced mantle convection, Nature 317, 135–139, 1985.
11 R.W. Scott and F.M. Govean, Early depositional history of a rift basin: Miocene in the western Sinai, Palaeogeogr. Palaeoclimatol., Palaeoecol. 52, 143–158, 1985.
12 Z. Garfunkel and Y. Bartov, The tectonics of the Suez Rift, Geol. Surv. Israel Bull. 71, 44 pp., 1977.
13 F. Berthelot, Etude thermique du Golfe de Suez dans son contexte géodynamique. 194 pp., These 3eme cycle, Université Paris 6, 1986.
14 D.J. Webster and N. Ritson, Post-Eocene stratigraphy of the Suez rift in S.W. Sinai, Egypt, E.G.P.C. 6th Exploration Seminar, Cairo, 16 pp., 1982.
15 B.P. Kohn and M. Eyal, History of uplift of the crystalline basement of Sinai and its relation to opening of the Red Sea as revealed by fission track dating of apatites, Earth Planet. Sci. Lett. 52, 129–141, 1981.
16 R. Freund, Z. Garfunkel, I. Zak, M. Goldberg, T. Weissbrod and B. Derin, The shear along the Dead Sea Rift, Philos. Trans. R. Soc. London, Ser. A 267, 107–130, 1970.
17 M. Eyal, Y. Eyal, Y. Bartov and G. Steinitz, The tectonic development of the western margin of the Gulf of Elat (Aqaba) rift, Tectonophysics 80, 39–66, 1981.

18 Z. Garfunkel, J. Bartov, Y. Eyal and G. Steinitz, Raham conglomerate-new evidence for Neogene tectonism in the southern part of the Dead Sea rift, Geol. Mag. 111, 55–64, 1976.

19 Z. Garfunkel, Internal structure of the Dead Sea leaky transform (rift) in relation to plate kinematics, Tectonophysics 80, 81–108, 1981.

20 Z. Ben-Avraham, G. Almagor and Z. Garfunkel, Sediments and structure of the Gulf of Elat (Aqaba), Northern Red Sea, Sediment. Geol. 23, 239–267, 1979.

21 R.J. Fleck, R.G. Coleman, H.R. Cornwall, W.R. Greenwood, D.G. Hadley, D.L. Schmidt, W.C. Prinz and J.C. Ratte, Geochronology of the Arabian Shield, western Saudi Arabia: K-Ar results, Geol. Soc. Am. Bull. 87, 9–21, 1976.

22 D.B. Stoeser and V.E. Camp, Pan-African microplate accretion of the Arabian Shield, Geol. Soc. Am. Bull. 96, 817–826, 1985.

23 A.H. Hashad, Present status of geochronological data on the Egyptian basement complex, in: Evolution and mineralization of the Arabian-Nubian shield, N.J. Jackson, ed., Vol. 3, pp. 31–46, 1980.

24 P. Morgan, D.D. Blackwell, J.C. Farris, F.K. Boulos and P.G. Salib, Preliminary geothermal gradient and heat flow values for northern Egypt and Gulf of Suez from oil well data, in: Proceedings of the International Congress on Thermal Waters, Geothermal Energy and Vulcanism of the Mediterranean Area, Vol. 1, pp. 424–438, Natl. Tech. Univ., Athens, 1977.

25 J. Makris, Z. Ben Avraham, A. Behle, A. Ginzberg, P. Giese, L. Steinmetz, R.B. Whitmarsh and S. Eleftheriou, Seismic refraction profiles between Cyprus and Israel and their interpretation, Geophys. J. R. Astron. Soc., pp. 575–591, 1983.

26 A. Bein and G. Gvirtzman, A mesozoic fossil edge of the Arabian plate along the Levant coastline and its bearing on the evolution of the Eastern Mediterranean, in: Structural History of the Mediterranean Basins, B. Diju-Duval and L. Montadert, eds., pp. 95–110, Editions Technip, Paris, 1977.

27 A. Ginzburg and G. Gvirtzman, Changes in the crust and in the sedimentary cover across the transition from the Arabian platform to the Mediterranean basin: evidence from seismic refraction and sedimentary studies in Israel and in Sinai, Sediment. Geol. 23, 19–36, 1978.

28 Z. Garfunkel and B. Derin, Permian-Early Mesozoic tectonism and continental margin formation in Israel and its implications for the history of the Eastern Mediterranean, in: The Geological Evolution of the Eastern Mediterranean, J.E. Dixon and A.H.F. Robertson, eds., Geol. Soc. Spec. Publ. 17, 187–201, 1985.

29 M.S. Steckler and A.B. Watts, Subsidence of the Atlantic type continental margin off New York, Earth Planet. Sci. Lett. 42, 1–13, 1978.

30 G. Gvirtzman and G. Steinitz, The Asher volcanics in northern Israel: an early Jurassic event (abstract), 1984 Annu. Meet., Isr. Geol. Soc., pp. 45–46, chart, 1984.

31 R. Freund, M. Goldberg, T. Weissbrod, Y. Druckman and B. Derin, The Triassic-Jurassic structure of Israel and its relations to the origin of the Eastern Mediterranean, Isr. Geol. Surv. Bull. 65, 26 pp., 1975.

32 A.B. Watts and M.S. Steckler, Subsidence and eustasy at the continental margin of eastern North America, Am. Geophys. Union, Maurice Ewing Ser. 3, 218–234, 1979.

33 R. Salem, Evolution of Eocene-Miocene sedimentation patterns in parts of northern Egypt, Am. Assoc. Pet. Geol. Bull. 60, 34–64, 1976.

34 A. Ginzburg, J. Makris, K. Fuchs, C. Prodehl, W. Kaminski and U. Amitai, A seismic study of the crust and upper mantle of the Jordan Dead Sea rift and their transition toward the Mediterranean Sea, J. Geophys. Res. 84, 1569–1582, 1979.

35 W.M. Meshref and M.M. El Sheikh, Magnetic-tectonic trend analysis in northern Egypt, Egypt. J. Geol., pp. 13–15, 1973.

36 Y. Folkman and Z. Yuval, Aeromagnetic Map of Israel, 3 sheets, Institute for Petroleum Research and Geophysics, Israel, 1976.

37 S. Riad, Shear zones in North Egypt interpreted from gravity data, Geophysics 42, 1207–1214, 1977.

38 Y. Folkman and R. Assael, Sinai Gravity Map, 1 sheet, Institute for Petroleum Research and Geophysics, Israel, 1980.

39 C. Goetze and B. Evans, Stress and temperature in the bending lithosphere as constrained by experiment rock mechanics, Geophys. J. R. Astron. Soc. 59, 463–478, 1979.

40 S.H. Kirby, Rheology of the lithosphere, Rev. Geophys. Space Phys. 21, 1458–1487, 1983.

41 C. Goetze, The mechanisms of creep in olivine, Philos. Trans. R. Soc. London, Ser. A 288, 99–119, 1978.

42 J.H. Bodine, M.S. Steckler and A.B. Watts, Observations of flexure and the rheology of the oceanic lithosphere. J. Geophys. Res. 86, 3695–3707, 1981.

43 W.D. Mooney, M.E. Gettings, H.R. Blank and J.H. Healy, Saudi Arabian seismic refraction profile: a travel time interpretation of crustal and upper mantle interpretation, Tectonophysics 111, 173–246, 1985.

44 P. Morgan and J.H. Sass, Thermal regime of the continental lithosphere, J. Geodyn. 1, 143–166, 1984.

45 A.B. Watts and J.A. Thorne, Tectonics, global changes in sea-level and their relationship to stratigraphic sequences at the U.S. Atlantic continental margin, Mar. Pet. Geol. 1, 319–339, 1984.

46 A. Ginzburg and Y. Folkman, The crustal structure between the Dead Sea rift and the Mediterranean Sea, Earth Planet. Sci. Lett. 51, 181–188, 1980.

47 C.A. Stein and J.R. Cochran, The transition between the Sheba ridge and Owen basin: rifting of old oceanic lithosphere, Geophys. J. R. Astron. Soc. 81, 47–74, 1985.

48 W.F. Brace and D.L. Kohlstedt, Limits on lithospheric stress imposed by laboratory experiments, J. Geophys. Res. 85, 6248–6252, 1980.

49 R. Meissner and J. Strehlau, Limits of stresses in continental crusts and their relation to the depth-frequency distribution of shallow earthquakes, Tectonics 1, 73–89, 1982.

50 N. Kuznir and R.G. Park, The extensional strength of the continental lithosphere: its dependence on geothermal gradient, crustal composition and crustal thickness (abstract), Extensional Tectonics Meet., Durham, England, April 1985.

51 R.B. Smith and R.L. Bruhn, Intraplate extensional tecton-

ics of the eastern Basin and Range: inferences on structural style from seismic data, regional tectonics and thermal-mechanical models of brittle/ductile deformation, J. Geophys. Res. 89, 5733–5762, 1984.
52 P. England, Constraints on extension of continental lithosphere, J. Geophys. Res. 88, 1145–1152, 1983.
53 D.S. Sawyer, Brittle failure in the upper mantle during extension of continental lithosphere, J. Geophys. Res. 90, 3021–3025, 1985.
54 J.K. Weissel and D.E. Hayes, Evolution of the Tasman Sea reappraised, Earth Planet. Sci. Lett. 36, 77–84, 1977.
55 O. Eldholm and J.C. Mutter, Basin structure of the Norwegian margin from analysis of digitally recorded sonobuoys, J. Geophys. Res., in press, 1986.
56 P. Barton and R. Wood, Tectonic evolution of the North Sea basin: crustal stretching and subsidence, Geophys. J. R. Astron. Soc. 79, 987–1022, 1984.
57 R. von Huene, M.A. Fisher, T.R. Bruns and G.G. Shor, Jr., Continental margins of the Gulf of Alaska and Late Cenozoic tectonic plate boundaries, in: Sisson, A. (ed.) The relationship of plate tectonics to Alaskan geology and resources, A. Sisson, ed., Symp. Proc., Alaska Geol. Soc., p. J-1-33, 1977.
58 T. Atwater, Implications of plate tectonics for the Cenozoic tectonic evolution of western North America, Geol. Soc. Am. Bull. 81, 3513–3566, 1970.
59 T.J. Fitch, Plate convergence, Transcurrent faults and internal deformation adjacent to Southeast Asia and the Western Pacific, J. Geophys. Res. 77, 4432–4460, 1972.
60 J.A. Katili, Volcanism and plate tectonics in the Indonesian island arcs, Tectonophysics 26, 165–188, 1974.
61 V.F. Cormier, Tectonics near the junction of the Aleution and Kuril-Kamchatka Arcs and a mechanism for Middle Tertiary magmatism in the Kamchatka basin, Geol. Soc. Am. Bull. 86, 443–453, 1975.
62 J.R. Curray, D.G. Moore, L.A. Lawver, F.J. Emmel, R.W. Raitt, M. Henry and R. Kieckhefer, Tectonics of the Andaman Sea and Burma, Am. Assoc. Pet. Geol. Mem. 29, 189–198, 1978.
63 D.E. Karig, Origin and development of marginal basins in the Western Pacific, J. Geophys. Res. 76, 2542–2561, 1971.
64 E.T. Degens et al., eds., The Black Sea-Geology, Chemistry and Biology, Am. Assoc. Pet. Geol. Mem. 20, 633 pp., 1974.
65 S. Joffe and Z. Garfunkel, Plate kinematics of the circum Red Sea—a reevaluation, Tectonophysics, in press, 1986.